Journal of the Nigerian Association of Mathematical Physics
Volume 52 (*July & Sept., 2019 Issue*), pp53 – 58

SECOND-ORDER NON-OSCILLATORY SCHEME FOR SIMULATING A PRESSURE-DRIVEN FLOW

Chinedu Nwaigwe[1] and Charles Orji[2]

[1]Department of Mathematics, Rivers State University, Port Harcourt, Nigeria
[2]Department of Marine Engineering, Rivers State University, Port Harcourt, Nigeria

Abstract

We propose a second-order finite difference scheme to study the flow of a viscous fluid in a stationary horizontal channel with porous walls. Following conservation principles, we obtain the governing equation in the form of a convection-diffusion problem. Naive discretization leads to either oscillatory solutions or low order accurate schemes. So second-order and non-oscillatory scheme is desirable. We use the idea of information propagation as indicated by the convective term. This informs the use of a backward discretization for first spatial derivative leading to a non-oscillatory second-order accurate scheme in space. The error estimates are obtained theoretically, and the method of manufactured solutions is adopted to verify the convergence of the method. The numerical results verify that the method is truly second-order in space, convergent and free of any numerical oscillations. We probe the effects of the model parameters on the flow and found that increasing the suction parameter decreases the magnitude of x-velocity component while increasing the pressure gradient increases the magnitude of x-velocity component.

1. Introduction

Understanding water flows in channels (closed and open) is very important due to their impact on man and environment. For example, flooding has caused the loss of over 500,000 lives and the damage of properties worth over twenty billion US dollars [1]. Such understanding can help to enhance evacuation during flood disasters, hence reduce the consequences on lives and properties. Flow understanding is also crucial in the design of drainage and other water supply systems. Therefore, studying the flow of fluids in channels remains an important research area. Computational fluid dynamics (CFD) has become an important approach to study fluid flows and related phenomena. Several applications of CFD are discussed in [2].

Hyperbolic shallow water models and conservative implicit method are developed for the study of both pipe and open channel flows in [3]. The numerical scheme is based on total variation diminishing methods. The performance of the model was tested in simplified looped pipe network and very good agreement was observed. Capart and collaborators [4] also carried out both numerical and experimental study of trans-critical flows in closed sewer pipes. They considered shock-capturing schemes and the numerical results were validated against experimental results. Other combined numerical and experimental studies of various flows are reported in [5, 6].

Bourdarias and Gerbi [7] proposed a dual model for pipe flows with both free surface and pressurized conditions. The interface between the two flow types is treated as a free boundary and a Roe-like conservative scheme is adapted. The numerical results are compared with experimental data obtained from a laboratory test, and the data was correctly reproduced. Malekpour and Karney [8] proposed a non-oscillatory Godunov-type scheme for pressurized pipe flows. The numerical results are verified using analytical solutions.

The Preissmann slot method is adapted in Fernndez-Pato and GarcaNavarro [9], see also [10], to formulate a finite volume model for the simulation of networks of unpressurized pipe flows with isolated pressurization. The validation is against both analytical solutions and experimental data. Nanofluids flow between parallel plates are considered in [11]. Recent studies concerning pipe flows can be found in [12-15], see also [16].

Corresponding Author**:** Chinedu N., Email: nwaigwe.chinedu@ust.edu.ng, Tel: +2348034485274

Here, we are interested in flows through closed channels with porous walls; drainages are examples. Such pressure driven porous-channel flows often result to convection-diffusion equations which are known to be intractable by naive numerical discretization [17-23]. In particular, naive high-order central schemes lead to oscillatory solutions and upwind methods are only first order accurate in space [24]. This justifies the need for high-oder methods that are non-oscillatory. Therefore, our goal in this paper is to formulate a channel flow model, propose a non-oscillatory, second-order scheme for the model, analyse and verify the scheme and use the implemented scheme to investigate the impact of flow parameters on the flow.

The rest of the paper is organised as follows: section 2 derives the fluid dynamics model while section 3 presents the numerical scheme and theoretically prove the accuracy. In section 4 we present the numerical experiments first to verify the convergence and its order, second to demonstrate the non-oscillatory property and lastly to investigate the effect of flow parameters on the flow. The paper is concluded in section 5.

2. Problem Formulation

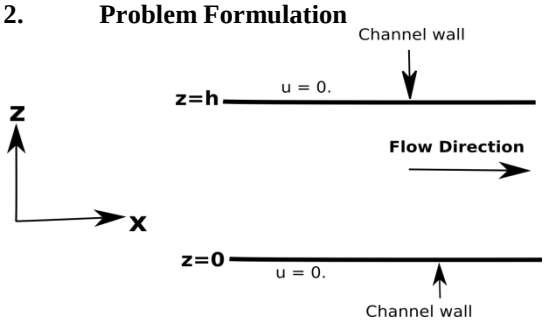

Figure 1: Physical set-up of Channel flow

Let $\rho, \epsilon, h, t_0, T, k \in \mathbb{R}, (z,t) \in \mathbb{R} \times \mathbb{R}^+$ and $u_* : \mathrm{R} \rightarrow \mathrm{R}$. Figure 1 depicts an infinitely long horizontal channel with the bottom and top walls at $z = 0$ and $z = h$ respectively. The walls are assumed porous. Assuming that fluid flows horizontally along the channel, the flow is driven by a constant pressure gradient, and there is no other external forces on the fluid. The lateral width of the channel is also assumed infinitely long so that the lateral walls have no effect on the flow. Further, we assume that a velocity (in the form of suction) of magnitude $w = \epsilon g(t)$ is directed towards the porous walls (along $z-$axis). The fluid is incompressible, Newtonian and has a unit kinematic viscosity, then by considering no-slip conditions on the walls and assuming that the initial velocity is $(u_*(z), 0, \epsilon g(t))$, the fluid velocity component u along the channel is governed by the following problem: find the unknown $u(z,t)$ such that:

$$\frac{\partial u(z,t)}{\partial t} + \epsilon g(t)\frac{\partial}{\partial z}u(z,t) = \frac{\partial^2}{\partial z^2}u(z,t) - \frac{1}{\rho}\frac{\partial P}{\partial x} + f(z,t), \quad z \in (0,h),\, t \in (0,T)$$
$$u(0,t) = u(h,t) = 0, \quad \forall t \in [0,T],$$
$$u(z,0) = u_*(z), \quad \forall z \in [0,h], \qquad (1)$$

where $0 \leq |g(t)| \leq g_{max} < \infty$, for all $t \in [0,T]$ and $f(z,t)$ represents the sum of all external forces acting on the fluid, here assumed to be zero. We included f in the model since the numerical scheme to be formulated in the next section will be for a general model including the sources f. In this study, we assume $g(t) = e^{-kt}$. We also define the pressure gradient term

$$P_x = \frac{1}{\rho}\frac{\partial P}{\partial x}$$

which is assumed constant. The constant shall be called the velocity parameter or suction parameter, while ρ is the fluid's constant density. Our goal is to design a numerical scheme for the problem (1) which is secondorder and free of numerical oscillations, and to understand the effects of the flow parameters on the flow.

3. Numerical Scheme

In order to apply the method of manufactured solutions [25, 26] for verifications, we formulate the numerical schemes for problem (1) in a more general form including a source term $f(z,t)$.

Let $M \in \mathrm{Z}^+; n = 0,1,2,\cdots$; and $i = 0,1,2,3,\cdots, M$. Define $\Delta z := h/M$ and Δt be given. We discretize the domain, $z_i = i\Delta z \forall i$, and in time $t^n = n\Delta t \forall n$, and let $u_i^n \approx u(x_i, t^n)$. The most delicate term to discretize in (1) is the convective term. It is known that a central discretization (though second order) leads to oscillatory solution and a simple upwind scheme is only first-order [24]. Here, we approach the problem following the fact that the convection coefficient is positive, hence we propose a second-order backward (upwind) discretization leading to the following numerical scheme:

$$\frac{u_i^{n+1}-u_i^n}{\Delta t}+\epsilon g(t^{n+1})\frac{u_{i-2}^{n+1}-4u_{i-1}^{n+1}+3u_i^{n+1}}{2\Delta z}=\frac{u_{i+1}^{n+1}-2u_i^{n+1}+u_{i-1}^{n+1}}{(\Delta z)^2}$$
$$-P_x+f(z_i,t^{n+1}) \qquad (2)$$

The above scheme is complimented with the following conditions:

$$\left.\begin{array}{ll} u_0^{n+1}=u_M^{n+1}=0 & \forall n \\ u_0^i=u_*(z_i) & \forall i \end{array}\right\} \qquad (3)$$

The scheme (2)-(3) form the complete numerical formulation. Before applying the scheme to simulate the flow, we first study its accuracy. Hence in the next sub-section we show that the scheme is second-order accurate in space and first-order in time.

3.1 Error Analysis

We define the truncation error, T_i^n for the scheme (2)-(3), as follows:

$$T_i^n=\frac{u(z_i,t^{n+1})-u(z_i,t_n)}{\Delta t}+\epsilon g(t^{n+1})\frac{u(z_{i-2},t^{n+1})-4u(z_{i-1},t^{n+1})+3u(z_i,t^{n+1})}{2\Delta z}$$
$$-\frac{u(z_{i+1},t^{n+1})-2u(z_i,t^{n+1})+u(z_{i-1},t^{n+1})}{(\Delta z)^2}+P_x-f(z_i,t^{n+1}),$$

Theorem 3.1 (Consistency)**.** *The truncation error, T_i^n satisfies:*

$$|T_i^n|\le\frac{\Delta t}{2}M_{tt}+\frac{(\Delta z)^2}{6}\left(6\epsilon g_{max}M_{zzz}+M_{zzzz}\right) \qquad (4)$$

for all n and for all i,

where g_{max}:= max$|g(t)|$,M_{tt}:= max$|u_{tt}(z,t)|$,M_{zzz}:= max$|u_{zzz}(z,t)|$ and M_{zzzz}:= max$|u_{zzzz}(z,t)|$ taking all over $(z,t)\in[0,1]\times[0,T]$. Note that subscript, z, indicates partial derivatives.

Proof. By the Taylor's theorem:

$$\frac{u(z_i,t^{n+1})-u(z_i,t^n)}{\Delta t}=u_t(z_i,t^{n+1})+\frac{\Delta t}{2}u_{tt}(z_i,q^{n+1}),\quad q^{n+1}\in(t^n,t^{n+1}).$$

$$\frac{u(z_{i-2},t^{n+1})-4u(z_{i-1},t^{n+1})+3u(z_i,t^{n+1})}{2\Delta z}$$
$$=u_x(z_i,t^{n+1})+\frac{(\Delta z)^2}{6}\left(-2u_{zzz}(\nu_1,t^{n+1})+4u_{zzz}(\nu_2,t^{n+1})\right),$$

$\nu_1\in(z_{i-1},z_i)$, $\nu_2\in(z_{i-2},z_i)$.

$$\frac{u(z_{i+1},t^{n+1})-2u(z_i,t^{n+1})+u(z_{i-1},t^{n+1})}{(\Delta z)^2}=u_{zz}(z_i,t^{n+1})$$
$$+\frac{(\Delta z)^2}{12}\left(u_{zzzz}(\mu_l,t^{n+1})+u_{zzzz}(\mu_r,t^{n+1})\right),\quad \mu_l\in(z_{i-1},z_i),\ \mu_r\in(z_i,z_{i+1}).$$

Hence,

$$\begin{aligned}T_i^n&=u_t(z_i,t^{n+1})+\epsilon g(t^{n+1})u_z(z_i,t^{n+1})-u_{zz}(z_i,t^{n+1})+P_x-f(z_i,t^{n+1})\\&=\frac{\Delta t}{2}u_{tt}(z_i,\rho^{n+1})+\epsilon e^{-kt^{n+1}}\frac{(\Delta z)^2}{6}\left(-2u_{zzz}(\nu_1,t^{n+1})+4u_{zzz}(\nu_2,t^{n+1})\right)\\&\quad-\frac{(\Delta z)^2}{12}\left(u_{zzzz}(\mu_l,t^{n+1})+u_{zzzz}(\mu_r,t^{n+1})\right)\\&\le\frac{\Delta t}{2}u_{tt}(z_i,q^{n+1})\\&\quad+\epsilon g(t^{n+1})\frac{(\Delta z)^2}{6}\left(2M_{zzz}+4M_{zzz}\right)\\&\quad-\frac{(\Delta z)^2}{12}\left(u_{zzzz}(\mu_l,t^{n+1})+u_{zzzz}(\mu_r,t^{n+1})\right)\\&\le\frac{\Delta t}{2}M_{tt}+\epsilon g_{max}\frac{(\Delta z)^2}{6}6M_{zzz}+\frac{(\Delta z)^2}{12}2M_{zzzz}\\&=\frac{\Delta t}{2}M_{tt}+\frac{(\Delta z)^2}{6}\left(6\epsilon g_{max}M_{zzz}+M_{zzzz}\right).\end{aligned}$$

Hence, the scheme is second order accurate in space and first order in time.

4. Numerical Results

This section presents some numerical experiments first to verify the convergence of the proposed scheme, next to we demonstrate the non-oscillatory property of the computed solutions by comparing with those of a central scheme and a

backward (upwind) scheme. Finally, we investigate the flow variations with the velocity parameter and the pressure gradient term P_x.Except otherwise stated, we investigate the results for $h = 0.2$ and $k = 0.5$.

In the next two sub-sections, we use the method of manufactured solutions to verify the convergence and non-oscillatory property of the method. To this end we consider the exact ("manufactured") solution derived in [24] which is given by

$$w(z,t) = \frac{P_x}{2}z(z-h) + \epsilon e^{-kt}\left(Acos(\sqrt{k}z) + Bsin(\sqrt{k}z) + \frac{P_x}{k}(z-\frac{h}{2})\right), \quad (5)$$

Where

$A = \frac{P_x h}{2k}$ and $B = \frac{\frac{P_x h}{2k}(1+\cos(h\sqrt{k}))}{\sin(h\sqrt{k})}$

This corresponds to the solution of problem (1) with a source term,

$$f(z,t) = \epsilon^2\sqrt{k}e^{-2kt}\left(Bcos(\sqrt{k}z) - Asin(\sqrt{k}z) + \frac{P_x}{k\sqrt{k}}\right),$$

and the initial condition: $u_*(z) = w(z,0)$.

4.1 Experimental Order of Convergence (EOC)

Here, we numerically verify the convergence (and its order) for the presented scheme. We set $\Delta t=0.005$, $\epsilon=100$, $P_x=1$, and the following number of grid points, 3×2^j for $j = 0,1,2,\cdots,10$. For each grid, we terminate the simulation after time $t = 0.5$, and also the errors (in2-norm). The errors and experimental order of convergence (eoc) are shown in table 1. It can be seen that the scheme is second-order in space as theoretically proven.

Table 1: Experimental Order of Convergence

No. of Grid Points	*Error*	*EOC*
4	0.00161095165193	-
8	0.000404379131977	1.9941327424973307
16	8.70609703385e-05	2.215610543856763
32	2.73347528001e-05	1.67128977109692
64	8.72271630915e-06	1.6478869542219423
128	2.48438228713e-06	1.811890282383399
256	6.61848390175e-07	1.9083145055951183
512	1.7092562467e-07	1.9531320784028479
1024	4.3716872774e-08	1.9671065892362483
2048	1.13601499531e-08	1.9442083250712603
4096	3.2223872909e-09	1.8177800748456838

4.2 Comparison with Other Methods

In this sub-section, we verify the non-oscillatory property of the method, comparing it with a central scheme and a backward (upwind) scheme. The exact solution is also the manufactured solution listed above in (5), see [24].

The numerical results computed with the scheme (2)-(3) and those of central and first-order backward schemes are displayed in figures 2-4 using 81, 41 and 21 grid points respectively. We can see that when 81 grid points (figure 2) are used, the proposed scheme and the central scheme highly agree with the exact solution, while the first-order backward scheme has the least accuracy. This is expected since the backward scheme is only first-order.

Then, we coarsen the grids by using only 41 grid points in figure 3 and see that the solution computed by the central scheme begins to develop numerical oscillations while those of the first-order backward scheme becomes much less accurate, but those of the proposed scheme remains both highly accurate and non-oscillatory.

We further coarsen the grid - using only 21 grid points - see figure 4. We can see clearly that the results computed by the central scheme gets highly oscillatory while that of the first-order backward scheme is poorly accurate. But the solution computed by the proposed scheme remains non-oscillatory while maintaining good accuracy. This verifies the **non-oscillatory** and **high accuracy** of the method.

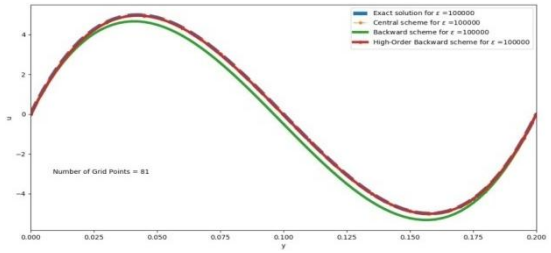

Figure 2: Comparison of schemes using 81 grid points

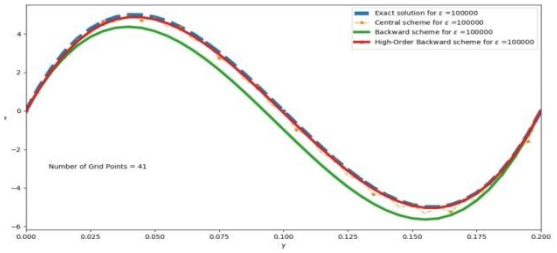

Figure 3: Comparison of schemes using 41 grid points

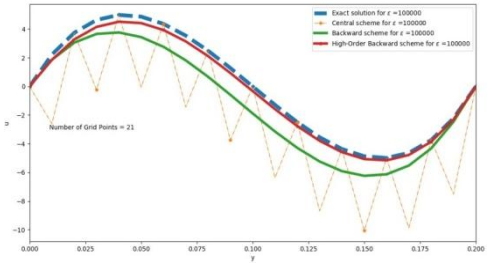

Figure 4: Comparison of schemes using 21 grid points

4.3 Flow Analysis

In this final sub-section, we investigate the influence of the flow parameters, and P_x, on the horizontal velocity components - see figures 5 and 6. The results are computed for problem (1) using $f = 0$ and $u_*(z) = w(z,0)$ with w given in (5). We can observe that increasing the velocity parameter decreases the velocity magnitude (see figure 5), while an increase in the pressure gradient increases the velocity magnitude (see figure figures 6). These are the expected results since the velocity parameter tends to direct the flow towards the vertical direction (towards the walls) hence should decrease the velocity along the channel. Also, the flow is driven by pressure gradient, so an increase in it will also increase the flow (velocity) and that is what is exactly reproduced by the numerical experiment in 6. We conclude that the numerical results correctly reproduced the expected physical results.

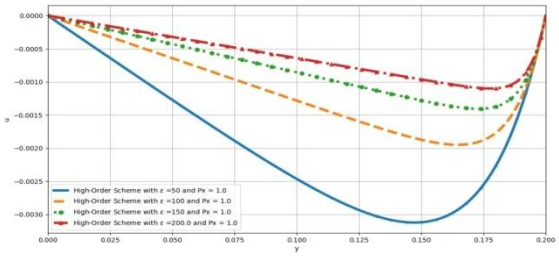

Figure 5: Variation of velocity with

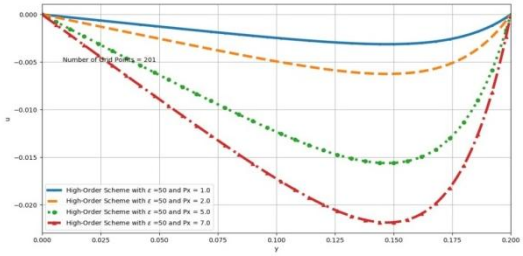

Figure 6: Variation of velocity with pressure gradient

We have formulated a channel flow model, derived a high-order scheme for the model and numerically demonstrated the non-oscillatory nature of the computed solutions. We also demonstrated that the scheme is convergent and that the flow increases with increasing pressure gradient but decreases with increasing suction/velocity parameter.

References

[1] S. Doocy, A. Daniels, S. Murray, and T. D. Kirsch. The human impact of floods: a historical review of events 1980-2009 and systematic. 2013.

[2] Mohd Hafiz Zawawi, A Saleha, A Salwa, NH Hassan, NazirulMubinZahari, MohdZakwan Ramli, and Zakaria Che Muda. A review: Fundamentals of computational fluid dynamics (cfd). In *AIP Conference Proceedings*, volume 2030, page 020252. AIP Publishing, 2018.

[3] P Garcia-Navarro, F Alcrudo, and A Priestley. An implicit method for water flow modelling in channels and pipes. *Journal of hydraulic research*, 32(5):721–742, 1994.

[4] H Capart, X Sillen, and Yves Zech. Numerical and experimental water transients in sewer pipes. *Journal of hydraulic research*, 35(5):659–672, 1997.

[5] Christophe Vall´ee, Thomas H¨ohne, Horst-Michael Prasser, and Tobias Su¨hnel. Experimental investigation and cfd simulation of horizontal air/water slug flow. *Kerntechnik*, 71(3):95–103, 2006.

[6] Christophe Vall´ee, Thomas H¨ohne, Horst-Michael Prasser, and Tobias Su¨hnel. Experimental investigation and cfd simulation of horizontal stratified two-phase flow phenomena. *Nuclear Engineering and Design*, 238(3):637–646, 2008.

[7] Christian Bourdarias and St´ephaneGerbi. A finite volume scheme for a model coupling free surface and pressurised flows in pipes. *Journal of Computational and Applied Mathematics*, 209(1):109–131, 2007.

[8] A Malekpour and B Karney. A non-oscillatory preissmann slot method based numerical model. *Procedia Engineering*, 89:1366–1373, 2014.

[9] J Fern´andez-Pato and P Garc´ıa-Navarro. A pipe network simulation model with dynamic transition between free surface and pressurized flow. *Procedia Engineering*, 70:641–650, 2014.

[10] J Fern´andez-Pato and P Garc´ıa-Navarro. Finite volume simulation of unsteady water pipe flow. *Drinking Water Engineering and Science*, 7(2):83–92, 2014.

[11] M Sheikholeslami, M Hatami, and G Domairry. Numerical simulation of two phase unsteady nanofluid flow and heat transfer between parallel plates in presence of time dependent magnetic field. *Journal of the Taiwan Institute of Chemical Engineers*, 46:43–50, 2015.

[12] Andreas Linkamp, Christian Deimel, Andreas Bruemmer, and Romuald Skoda. Non-reflecting coupling method for one-dimensional finite difference/finite volume schemes based on spectral error analysis. *Computers & Fluids*, 140:334–346, 2016.

[13] Jintao Liu, Shaohui Zhang, Di Xu, Meijian Bai, and Qunchang Liu. Coupled simulation and validation with fully implicit time scheme for free-surface-pressurized water flow in pipe/channel. *Transactions of the Chinese Society of Agricultural Engineering*, 33(19):124–130, 2017.

[14] Javier Fern´andez-Pato and Pilar Garc´ıa-Navarro. Development of a new simulation tool coupling a 2d finite volume overland flow model and a drainage network model. *Geosciences*, 8(8):288, 2018.

[15] Yanmei Wang, Chengcai Zhang, Zhansong Li, Bin Sun, and Haolan Zhou. Applicability of preissmann box scheme for calculation of transcritical flow in pipes. *Water Supply*, 2019.

[16] Chinedu Nwaigwe. *Sequential Implicit Numerical Scheme for Pollutant and Heat Transport in a Plane-Poiseuille Flow*. In print - Journal of Applied and Computational Mechanics, 2019.

[17] Aleksandr AndreevichSamarskii. *The theory of difference schemes*. New York: Marcel Dekker, 2001.

[18] PN Vabishchevich and MV Vasileva. Explicit-implicit schemes for convectiondiffusionreaction problems. *Numerical Analysis and Applications*, 15(4):359369, 2012.

[19] Willem Hundsdorfer and Jan G. Verwer. *Numerical solution of timedependent advection-diffusion-reaction equations*. Springer Science and Business Media, 2013.

[20] NdivhuwoMphephu. Numerical solution of 1-d convection-diffusionreaction equation. Master's thesis, University of Pretoria, South Africa, 2013.

[21] Lisha Wang and L-IW Roeger. Nonstandard finite difference schemes for a class of generalized convection–diffusion–reaction equations. *Numerical Methods for Partial Differential Equations*, 31(4):1288–1309, 2015.

[22] KC Patidar. Nonstandard finite difference methods: recent trends and further developments. *Journal of Difference Equations and Applications*, 22(6):817–849, 2016.

[23] HS Shekarabi and J Rashidinia. Three level implicit tension spline scheme for solution of convection-reaction-diffusion equation. *Ain Shams Engineering Journal*, 9:16011610, 2018.

[24] Chinedu Nwaigwe. *Analysis of Two Difference Schemes for Channel Flow Model with a Parameter*. In Review.

[25] KambizSalari and Patrick Knupp. Code verification by the method of manufactured solutions. Technical report, Sandia National Labs., Albuquerque, NM (US); Sandia National Labs , 2000.

[26] Patrick J Roache. The method of manufactured solutions for code verification. In *Computer Simulation Validation*, pages 295–318. Springer, 2019.